

Learning Sparse Graphs for Prediction and Filtering of Multivariate Data Processes

Arun Venkitaraman and Dave Zachariah

Abstract—We address the problem of prediction and filtering of multivariate data process using an underlying graph model. We develop a method that learns a sparse partial correlation graph in a tuning-free and computationally efficient manner. Specifically, the graph structure is learned recursively without the need for cross-validation or parameter tuning by building upon a hyperparameter-free framework. Experiments using real-world datasets show that the proposed method offers significant performance gains in prediction and filtering tasks, in comparison with the graphs frequently associated with these datasets.

I. INTRODUCTION

Complex data-generating processes are often described using graph models [1], [2]. In such models, each node represents a component with a signal. Directed links between nodes represent their influence on each other. For example, in the case of sensor networks, a distance-based graph is often used to characterize the underlying process [3]. In this paper, we are interested in graph models that are useful for prediction and filtering tasks. In the former case, the goal is to predict the signal values at a subset of nodes using information from the remaining nodes. In the latter case, the observed signal has been subject to some unknown perturbation and the goal is to identify the magnitude and source nodes of the perturbation [4]. To address both tasks, we aim to learn partial correlation graph models from a finite set of training data. Such graphs can be viewed as the minimal-assumption counterparts of conditional independence graphs [5], [6]. In the special case of Gaussian signals, the latter collapses into the former.

As the size of the graph grows, the number of possible links between nodes grows quadratically. Thus to learn all possible links in a graph model requires large quantities of data. In many naturally occurring and human-made processes, however, the signal values at one node can be accurately predicted from a small number of other nodes. That is, there exists a corresponding sparse graph such the links to each node are few, directly connecting only a small subset of the graph [7]. By taking sparsity into account it is possible to learn graph models with good predictive properties from far fewer samples. The methods for learning sparse models are usually posed as optimization problems and face two major challenges here. First, they require several hyperparameters to specify the appropriate sparsity-inducing constraints as shown below. Second, both tuning hyperparameters and solving the associated optimization problem is often computationally intractable and must be repeated each time the training dataset is augmented by a new data snapshot.

The contribution is a method for learning sparse partial correlation graph for prediction and filtering that achieves two goals:

- obviates the need to specify and tune hyperparameters.
- computationally efficient with respect to the training data size.

The resulting prediction and filtering properties are demonstrated using real and synthetic datasets.

Reproducible research: Code for the method is available at <https://github.com/dzachariah/sparse-pcg>

II. PROBLEM FORMULATION

We consider a weighted directed graph with nodes indexed by set $\mathcal{V} = \{1, 2, \dots, P\}$. Let x_i denote a signal at the i th node and the link from node j to i has a weight w_{ij} . The signals from all nodes are collected in a P -dimensional vector $\mathbf{x} \sim p_0(\mathbf{x})$, where $p_0(\mathbf{x})$ is an unknown data generating process. We assume that its covariance matrix is full rank and, without loss of generality, consider the signals to be zero-mean. Next, we define the weights and related target quantities.

A. Partial correlation graph

A partial correlation graph is a property of $p_0(\mathbf{x})$ and can be derived as follows. Let

$$\begin{aligned}\tilde{x}_i &= x_i - \text{Cov}[x_i, \mathbf{x}_{-i,-j}] \text{Cov}[\mathbf{x}_{-i,-j}]^{-1} \mathbf{x}_{-i,-j} \\ \tilde{x}_j &= x_j - \text{Cov}[x_j, \mathbf{x}_{-i,-j}] \text{Cov}[\mathbf{x}_{-i,-j}]^{-1} \mathbf{x}_{-i,-j}\end{aligned}\quad (1)$$

denote the innovations at node i and j after partialling out the signals from all other nodes, contained in vector $\mathbf{x}_{-i,-j}$ [8]. The weight of the link from node j to node i is then defined as

$$w_{ij} \triangleq \frac{\text{Cov}[\tilde{x}_i, \tilde{x}_j]}{\text{Var}[\tilde{x}_j]}, \quad (2)$$

which quantifies the direct effect of node j on node i . In many applications, we expect only a few links incoming to node i to have nonzero weights w_{ij} .

The graph structure is thus encoded in a $P \times P$ weighted adjacency matrix \mathbf{W} , where the ij th element is equal to w_{ij} and the diagonal elements are all zero. This enables us to write a compact signal representation associated with the graph. First, at node i define a latent variable $\varepsilon_i = x_i - \sum_{j \neq i} w_{ij} x_j$. By re-arranging, we can simply write

$$\mathbf{x} = \mathbf{W}\mathbf{x} + \boldsymbol{\varepsilon}, \quad (3)$$

where $\boldsymbol{\varepsilon}$ has zero mean by construction. Moreover, the i th element ε_i belongs to the linear space spanned by x_i and

\mathbf{x}_{-i} . That is, $\varepsilon_i \in \mathcal{L}(x_i, \mathbf{x}_{-i})$, cf. [8, ch. 3]. We note that the subspace $\mathcal{L}(\mathbf{x}_{-i})$ can be jointly spanned by innovations $\tilde{x}_j, \forall j \neq i$ and that $\varepsilon_i \perp \tilde{x}_j$. Thus ε_i does not lie in the subspace $\mathcal{L}(\mathbf{x}_{-i})$ and for each row in (3), the latent variable is uncorrelated with the other signals: $\varepsilon_i \perp \mathbf{x}_{-i}$.

B. Target quantities

Having defined the weighted graph above, we now turn to the problem of prediction and filtering of data processes.

- 1) *Prediction*: Given a signal \mathbf{x}_0 from a subset of nodes $\mathcal{V}_0 \subset \mathcal{V}$, the problem is to predict unknown signal values at the remaining nodes \mathcal{V}_* . A natural predictor of \mathbf{x}_* is then:

$$\hat{\mathbf{x}}_*(\mathbf{W}) = \mathbf{W}_{*,0}\mathbf{x}_0, \quad (4)$$

where $\mathbf{W}_{*,0}$ denotes the corresponding submatrix of \mathbf{W} of size $|\mathcal{V}_*| \times |\mathcal{V}_0|$.

- 2) *Filtering*: Suppose that the signal at one or more nodes is subject to an unknown perturbation $\boldsymbol{\delta}$, which is identifiable when $\mathbf{I}_P - \mathbf{W}$ is full rank. Then (3) has an equivalent representation $\mathbf{x} = (\mathbf{I}_P - \mathbf{W})^{-1}\boldsymbol{\varepsilon}$ and the perturbed signals can be written as $\tilde{\mathbf{x}} = (\mathbf{I}_P - \mathbf{W})^{-1}(\boldsymbol{\delta} + \boldsymbol{\varepsilon})$. An unbiased estimator of the perturbation can then be expressed as:

$$\hat{\boldsymbol{\delta}}(\mathbf{W}) = (\mathbf{I}_P - \mathbf{W})\tilde{\mathbf{x}}. \quad (5)$$

In both problems, the respective target quantities (4) and (5) are functions of \mathbf{W} .

Next, we develop a method for learning \mathbf{W} from a dataset

$$\mathcal{D} = \{\mathbf{x}(1), \mathbf{x}(2), \dots, \mathbf{x}(N)\},$$

where $\mathbf{x}(n)$ denotes the n th realization from $p_0(\mathbf{x})$. The learned graph $\hat{\mathbf{W}}$ is then used to evaluate the target quantities.

III. LEARNING A SPARSE GRAPH

Let the vector \mathbf{w}_i^\top be the i th row of \mathbf{W} after removing the corresponding diagonal element. Then, for snapshot n , we may express i th row of (3) as

$$x_i(n) = \underbrace{\mathbf{w}_i^\top \mathbf{x}_{-i}(n)}_{\triangleq \hat{x}_i(n; \mathbf{w}_i)} + \varepsilon_i(n), \quad (6)$$

where the variance of $\varepsilon_i(n)$ is denoted as σ_i^2 .

A natural approach to learn a sparse graph \mathbf{W} from N training samples is:

$$\min_{\mathbf{W}: \|\mathbf{w}_i\|_0 \leq K_i, \forall i} \sum_{i=1}^P \sum_{n=1}^N |x_i(n) - \hat{x}_i(n; \mathbf{w}_i)|^2 \quad (7)$$

where the constraint $\|\mathbf{w}_i\|_0 \leq K_i \ll P$ restricts the maximum number of directed links to each node. Let learned weights be denoted as \mathbf{w}_i^0 , then $\hat{x}_i(n; \mathbf{w}_i^0)$ is a sparse predictor of $x_i(n)$ which we take as a reference. While this learning approach leads to strictly sparse weights, it has two drawbacks. First, (7) is known to be NP-hard, and hence convex relaxations must be used practice [9]. Second, a user must specify suitable

bounds $\{K_i\}$. Tractable convex relaxations of (7), such as the ℓ_1 -penalized LASSO approach [4], [10]

$$\min_{\mathbf{W}} \sum_{i=1}^P \sum_{n=1}^N |x_i(n) - \hat{x}_i(n; \mathbf{w}_i)|^2 + \lambda_i \|\mathbf{w}_i\|_1, \quad (8)$$

avoid an explicit choice of $\{K_i\}$ but must in turn tune a set of hyperparameters $\{\lambda_i\}$ since neither K_i nor the variances σ_i^2 are not uniform in general. With the appropriate choice of λ_i , the resulting deviation of $\hat{x}_i(n; \hat{\mathbf{w}}_i)$ from $\hat{x}_i(n; \mathbf{w}_i^0)$ can be bounded [11]. Tuning these hyperparameters with e.g. cross-validation [12] is however computationally intractable, especially when N becomes large.

An alternative approach is to treat the weight vector \mathbf{w}_i as a random variable, with an expected value $\mathbf{0}$, prior to observing data from the i th node. Specifically, consider (6) conditioned on data from all other nodes $\mathbf{X}_{-i} = [\mathbf{x}_{-i}^\top(1) \cdots \mathbf{x}_{-i}^\top(N)]^\top$ and assume that

$$\mathbb{E}[\mathbf{w}_i | \mathbf{X}_{-i}] = \mathbf{0} \quad \text{and} \quad \text{Cov}[\mathbf{w}_i | \mathbf{X}_{-i}] = \text{diag}(\boldsymbol{\pi}_i),$$

where $\boldsymbol{\pi}_i$ is a vector of variances. Under this conditional model, the MSE-optimal estimator of \mathbf{w}_i after observing data from the i th node $\mathbf{x}_i = [x_i(1), \dots, x_i(N)]^\top$ is can be expressed as [8]:

$$\hat{\mathbf{w}}_i(\boldsymbol{\pi}, \sigma^2) = (\mathbf{X}_{-i}^\top \mathbf{X}_{-i} + \sigma^2 \text{diag}(\boldsymbol{\pi}))^{-1} \mathbf{X}_{-i}^\top \mathbf{x}_i. \quad (9)$$

Similar to the Empirical Bayes approach in [13], the hyperparameters $\boldsymbol{\pi}$ and σ^2 for each i can be estimated by fitting the marginalized covariance model

$$\text{Cov}[\mathbf{x}_i | \mathbf{X}_{-i}] = \mathbf{X}_{-i} \text{diag}(\boldsymbol{\pi}) \mathbf{X}_{-i}^\top + \sigma^2 \mathbf{I}_N$$

to the sample covariance $\widehat{\text{Cov}}[\mathbf{x}_i | \mathbf{X}_{-i}] = \mathbf{x}_i \mathbf{x}_i^\top$ [14], [15]. It was shown in [16], that evaluating (9) at the estimated hyperparameters is equivalent to solving a convex, weighted square-root LASSO problem:

$$\hat{\mathbf{w}}_i(\hat{\boldsymbol{\pi}}, \hat{\sigma}^2) = \arg \min_{\mathbf{w}_i} \|\mathbf{x}_i - \mathbf{X}_{-i} \mathbf{w}_i\|_2 + \sum_{j \neq i} \frac{\|\mathbf{x}_j\|_2}{\sqrt{N}} |w_{ij}|, \quad (10)$$

This problem (aka. SPICE) can be solved recursively with a runtime that scales as $\mathcal{O}(NP^2)$ [17]. Since each $\hat{\mathbf{w}}_i$ can be computed in parallel, this can be exploited to obtain $\hat{\mathbf{W}}$ in the same runtime order. Moreover, under fairly general conditions, the deviation of $\hat{x}_i(n; \hat{\mathbf{w}}_i)$ from $\hat{x}_i(n; \mathbf{w}_i^0)$ is bounded by known constants [18].

In sum, using the SPICE approach (10) we learn a sparse graph $\hat{\mathbf{W}}$ in a statistically motivated and computationally efficient manner without the need to search for or tune hyperparameters.

IV. EXPERIMENTS

We apply the learning method to both synthesized and real-world multivariate data. We use a training set consisting of N samples to learn a sparse graph. Then by evaluating target quantities (4) and (5) at $\hat{\mathbf{W}}$, we perform prediction and filtering on separate testing sets. For the real data, filtering experiments were not considered since they require obtaining test signals with known perturbations.

The performance is quantified using normalized mean-squared error evaluated over a test set. Specifically, we define the normalized prediction and filtering errors as

$$\text{NPE} = \frac{\mathbb{E} [\|\mathbf{x}_* - \hat{\mathbf{x}}_*\|_2^2]}{\mathbb{E} [\|\mathbf{x}_*\|_2^2]} \quad \text{and} \quad \text{NFE} = \frac{\mathbb{E} [\|\boldsymbol{\delta} - \hat{\boldsymbol{\delta}}\|_2^2]}{\mathbb{E} [\|\boldsymbol{\delta}\|_2^2]},$$

respectively, where \mathbb{E} denotes the expectation operator. We evaluate the performance as a function of training set size N . The data is made zero-mean by subtracting the component-wise mean from the training and testing sets in all the examples considered.

A. Synthesized graphs

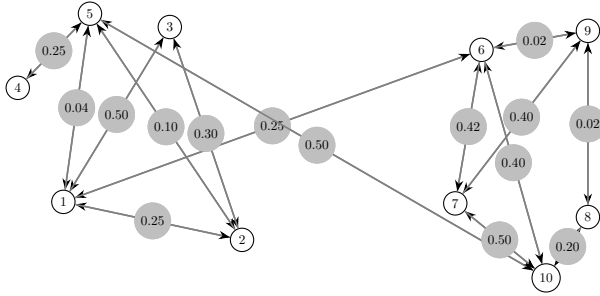


Fig. 1. Graph structure with nonzero weights defined by \mathbf{W} .

We consider the graph shown in Figure 1 with the indicated edge weights w_{ij} and is akin to a stochastic block model [19]. It consists of two densely connected communities of 5 nodes each with only two inter-community edges. To simulate network signals, we generate data as $\mathbf{x}(n) = (\mathbf{I}_P - \mathbf{W})^{-1} \boldsymbol{\varepsilon}(n)$. The elements of $\boldsymbol{\varepsilon}(n)$ were mutually uncorrelated and drawn from a Gaussian distribution with variances assigned as $\sigma_i^2 \in [0, 1]$ uniformly. We generate a total of 2×10^4 samples from which one half is used for training and the remaining for testing by partitioning the total dataset randomly. All the results are reported by averaging over 500 Monte Carlo simulations.

For sake of illustration, we include an example of $\hat{\mathbf{W}}$ from (10) when using training data of size $N = 10^4$ samples in Fig. 2(a). We begin by considering prediction task based using signals at nodes $\mathcal{V}_0 = \{2, 4, 6, 8, 10\}$ to predict the signals at nodes $\mathcal{V}_* = \{1, 3, 5, 7, 9\}$. Fig. 2(b) shows that NPE decreases with N and ultimately converges to the predictions of using the unknown \mathbf{W} .

The filtering task is performed by considering perturbations at nodes 1 and 10, since they are nodes with largest number of edges from each community. We perturb the values in the test set by adding a factor corresponding to five times the original values of $\varepsilon_i(n)$ at the nodes 1 and 10. We observe from Fig. 2(c) that the NFE reduces as N increases but does not reach the oracle limit. In Fig. 2(d) we observe the rate of overall improvement of the learned graph as N increases, measured as the normalized MSE $\mathbb{E}[\|\mathbf{W} - \hat{\mathbf{W}}\|_F^2]$.

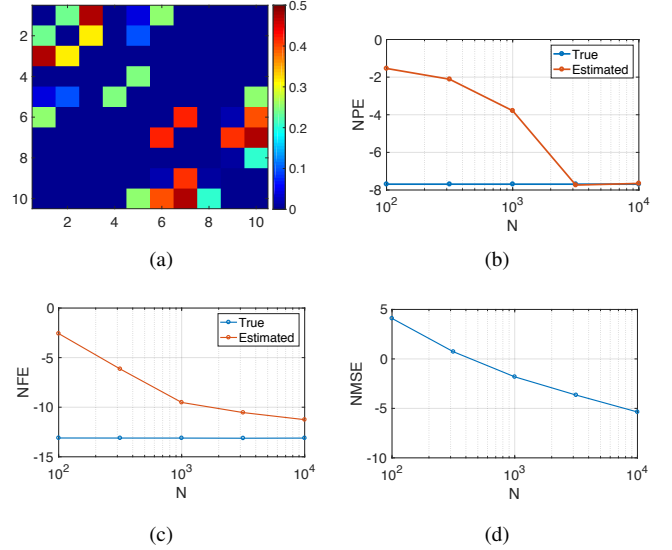


Fig. 2. Results for synthesized graph. (a) Example of learned graph $\hat{\mathbf{W}}$. (b) Prediction errors in [dB]. (c) Filtering errors in [dB]. (d) Normalized error of learned graph in [dB].

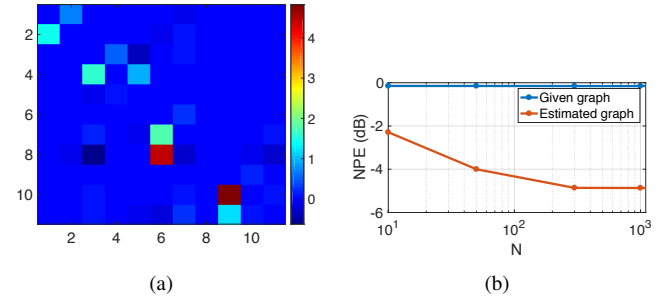


Fig. 3. Results for flow-cytometry data: (a) Learned graph $\hat{\mathbf{W}}$. (b) Prediction error in [dB].

B. Flow-cytometry data

We next consider flow-cytometry data used in [20], which consists of various instances of measurement of multiple phosphorylated protein and phospholipid components in thousands of individual primary human immune system cells. The data consists of total 7200 responses of $P = 11$ molecules to different perturbations which we divide the data into training and test sets. The partition is randomized and for each realization a graph \mathbf{W} is learned. A learned graph is illustrated in Fig. 3(a) using $N = 3600$ samples. For the prediction task, we evaluate the performance using 100 Monte Carlo repetitions and for sake of comparison we also evaluate the performance with the sparse binary directed graph \mathbf{W}' proposed in [20]. Though it was not designed for prediction it encodes the directed dependencies between nodes. We observe signals at nodes $\mathcal{V}_0 = \{3, 8, 9\}$, noting that these proteins have the maximum number of connections in \mathbf{W}' . Prediction is performed with respect to the remaining nodes $\mathcal{V}_* = \{1, 2, 4, 5, 6, 7, 10, 11\}$. We observe from Figure 3(b) that the learned partial correlation graph $\hat{\mathbf{W}}$ yields superior predictive performance when compared with that of the reference graph \mathbf{W}' . The improvements saturate beyond $N = 10^3$ samples.

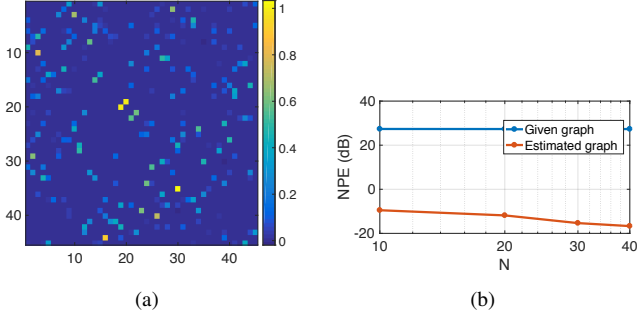


Fig. 4. Results for temperature data: (a) Learned graph $\widehat{\mathbf{W}}$. (b) Prediction error in [dB].

C. Temperature data for cities in Sweden

We next consider temperature data from the 45 most populated cities in Sweden. The data consists of 62 daily temperature readings for the period of November to December 2016 obtained from the Swedish Meteorological and Hydrological Institute [21]. In Fig. 4, we show a learned graph \mathbf{W} using $N = 30$ observations which is found to be sparse as expected.

For the prediction task, we use a subset of N observations for training and the remaining samples for testing, using 100 Monte Carlo repetitions. For reference, we compare the prediction performances with a distance-based graph \mathbf{W}' with elements

$$w'_{ij} = \begin{cases} \exp\left(\frac{-d_{ij}^2}{\sum_{i,j} d_{ij}^2}\right), & \forall i \neq j \\ 0 & i = j \end{cases} \quad (11)$$

where d_{ij} denotes the geodesic distance between the i th and j th cities. This graph structure is commonly used in modelling relations between data points in spectral graph analysis and in the recently popular framework of graph signal processing [22], which makes it a relevant reference.

The cities are ordered in descending order of their population and use the temperatures of the bottom 40 cities to predict the top 5 cities. That is, $\mathcal{V}_0 = \{1, 2, 3, 4, 5\}$ and $\mathcal{V}_* = \{6, \dots, 45\}$. In Fig. 4, we observe that the predictive performance using the learned graph $\widehat{\mathbf{W}}$ is high already at $N = 10$ samples while using reference graph does not provide a meaningful predictor.

D. 64-channel EEG data

Finally, we consider 64-channel electroencephalogram (EEG) signals obtained by placing 64 electrodes at various positions on the head of a subject and recorded different time-instants [23]. We divide the data consisting of 7000 samples into training and test sets using 100 Monte Carlo repetitions. An example of a learned graph is show in Fig. 5(a).

For reference, we compare the prediction performance when using a diffusion-based graph \mathbf{W}' , where

$$w'_{ij} = \exp\left(-\frac{\|\mathbf{r}_i - \mathbf{r}_j\|_2^2}{\sum_{i,j} \|\mathbf{r}_i - \mathbf{r}_j\|_2^2}\right),$$

and \mathbf{r}_j is the vector of 500 successive signal samples from a separate set of EEG signals at the j th electrode or node.

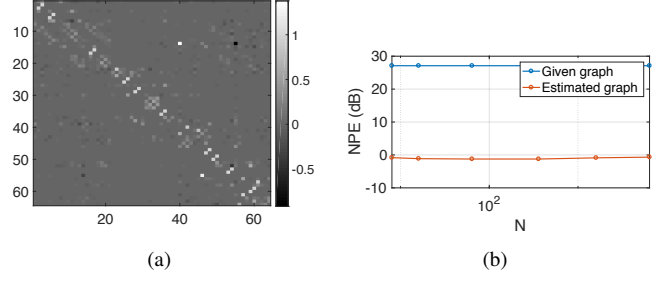


Fig. 5. Results for EEG data: (a) Learned graph $\widehat{\mathbf{W}}$. (b) Prediction error in [dB].

In Fig. 5(b) we observe that predictive performance using the learned partial correlation graph is substantially better than using the diffusion-based reference graph. Note however that EEG signals are typically. In particular, they exhibit has bursts of activation when a particular sensory task is initiated and this may not be well predicted even with a large amount of training data [24].

V. CONCLUSION

We have addressed the problem of prediction and filtering of multivariate data process by defining underlying graph model. Specifically, we formulated a sparse partial correlation graph model and two associated target quantities for prediction and filtering, respectively. The graph structure is learned recursively without the need for cross-validate or parameter tuning by building upon a hyperparameter-free framework. Using real-world data we showed that the learned partial correlation graphs offer superior prediction performance compared with standard weighted graphs associated with the datasets.

REFERENCES

- [1] E. D. Kolaczyk, *Statistical Analysis of Network Data: Methods and Models*. Springer Berlin, 2009.
- [2] *Network Science*. Cambridge Univ. Press, 2012.
- [3] D. I. Shuman, S. Narang, P. Frossard, A. Ortega, and P. Vandergheynst, "The emerging field of signal processing on graphs: Extending high-dimensional data analysis to networks and other irregular domains," *IEEE Signal Process. Mag.*, vol. 30, no. 3, pp. 83–98, 2013.
- [4] S. Yang and E. D. Kolaczyk, "Target detection via network filtering," *IEEE Transactions on Information Theory*, vol. 56, pp. 2502–2515, May 2010.
- [5] D. Koller and N. Friedman, *Probabilistic Graphical Models*. MIT Press, 2009.
- [6] A. A. Amini, B. Aragam, and Q. Zhou, "Partial correlation graphs and the neighborhood lattice," *ArXiv e-prints*, Nov. 2017.
- [7] D. Angelosante and G. B. Giannakis, "Sparse graphical modeling of piecewise-stationary time series," *Proc. IEEE Int. Conf. Acoust., Speech Signal Process.*, pp. 1960–1963, May 2011.
- [8] T. Kailath, A. H. Sayed, and B. Hassibi, *Linear estimation*. Prentice-Hall, Inc., 2000.
- [9] D. L. Donoho, M. Elad, and V. N. Temlyakov, "Stable recovery of sparse overcomplete representations in the presence of noise," *IEEE Trans. Inf. Theor.*, vol. 52, pp. 6–18, Jan. 2006.
- [10] R. Tibshirani, "Regression shrinkage and selection via the lasso," *Journal of the Royal Statistical Society, Series B*, vol. 58, pp. 267–288, 1994.
- [11] P. Bühlmann and S. Van De Geer, *Statistics for high-dimensional data: methods, theory and applications*. Springer Science & Business Media, 2011.
- [12] T. Hastie, R. Tibshirani, and J. Friedman, *The Elements of Statistical Learning: Data Mining, Inference, and Prediction, Second Edition*. Springer Series in Statistics, Springer New York, 2009.

- [13] J. Berger, *Statistical Decision Theory and Bayesian Analysis*. Springer Series in Statistics, Springer, 1985.
- [14] T. W. Anderson, "Linear latent variable models and covariance structures," *Journal of Econometrics*, vol. 41, no. 1, pp. 91–119, 1989.
- [15] P. Stoica, P. Babu, and J. Li, "New method of sparse parameter estimation in separable models and its use for spectral analysis of irregularly sampled data," *IEEE Trans. Signal Processing*, vol. 59, no. 1, pp. 35–47, 2011.
- [16] P. Stoica, D. Zachariah, and J. Li, "Weighted SPICE: A unifying approach for hyperparameter-free sparse estimation," *Digital Signal Processing*, vol. 33, pp. 1–12, 2014.
- [17] D. Zachariah and P. Stoica, "Online hyperparameter-free sparse estimation method," *IEEE Trans. Signal Processing*, vol. 63, pp. 3348–3359, July 2015.
- [18] D. Zachariah, P. Stoica, and T. B. Schön, "Online learning for distribution-free prediction," *arXiv preprint arXiv:1703.05060*, 2017.
- [19] M. E. J. Newman, *Networks: An Introduction*. Oxford University Press, 2010.
- [20] K. Sachs, O. Perez, D. Pe'er, D. A. Lauffenburger, and G. P. Nolan, "Causal protein-signaling networks derived from multiparameter single-cell data," *Science*, vol. 308, no. 5721, pp. 523–529, 2005.
- [21] "Swedish Meteorological and Hydrological Institute (SMHI)."
- [22] A. Sandryhaila and J. M. F. Moura, "Discrete signal processing on graphs," *IEEE Trans. Signal Process.*, vol. 61, no. 7, pp. 1644–1656, 2013.
- [23] A. L. Goldberger, L. A. N. Amaral, L. Glass, J. M. Hausdorff, P. C. Ivanov, R. G. Mark, J. E. Mietus, G. B. Moody, C.-K. Peng, and H. E. Stanley, "Physiobank, physiotoolkit, and physionet," vol. 101, no. 23, pp. e215–e220, 2000.
- [24] J. A. C. S. Sanei, *EEG Signal Processing*. Wiley, 2007.